Influence of Molten Salts on Soybean Oil Catalytic Pyrolysis with/without a Basic Catalyst

ARTICLE *in* ENERGY & FUELS · DECEMBER 2013

Impact Factor: 2.79 · DOI: 10.1021/ef4015845

5 AUTHORS, INCLUDING:

Jianli Wang

Zhejiang University of Technology

41 PUBLICATIONS **537** CITATIONS

energy&fuels

Article

pubs.acs.org/EF

Influence of Molten Salts on Soybean Oil Catalytic Pyrolysis with/without a Basic Catalyst

Guodong Zhang,[†] Fengwen Yu,*[,†] Weijin Wang,[†] Jianli Wang,[‡] and Jianbing Ji[†]

[†]Zhejiang Province Key Laboratory of Biofuel, College of Chemical Engineering and Materials Science, and [‡]Zhejiang Province Key Laboratory of Biofuel, The State Key Laboratory Breeding Base of Green Chemistry-Synthesis Technology, Zhejiang University of Technology, Hangzhou 310014, People's Republic of China

Supporting Information

ABSTRACT: The $ZnCl_2$–KCl molten salt mixture was used as the catalyst in soybean oil pyrolysis. The thermogravimetric (TG) experiments showed that the reaction pathway of soybean oil pyrolysis could be changed in the presence of molten salts. Moreover, the catalytic pyrolysis experiments were conducted in a laboratory-scale continuous stirred tank reactor (1.5 L). CaO was added to the molten salt mixture as a basic catalyst. The influence of the reaction temperature along with the CaO catalyst on molten salt pyrolysis of soybean oil was studied. The data of non-catalytic pyrolysis was also listed to explain the roles of molten salts and CaO catalyst. The results revealed that the $ZnCl_2$–KCl molten salt mixture had a unique performance in producing diesel-like fuels. The hydrocarbons were the main part of the bio-oil, which accounted for more than 80 wt %. The acid value was 3.9 mg of KOH/g at 40 g (5 wt % to the 800 g molten salt mixture) of CaO catalyst.

1. INTRODUCTION

The increasing consumption of fossil fuels is causing urgent environmental problems throughout the world.[1] In recent studies, oils derived from renewable resources can be used to produce biofuels via catalytic pyrolysis processes. The final products are similar in composition to that of diesel fuel and, thus, can be used in conventional engines without adaption.[2−7]

Currently, the choice of catalyst is the most important issue in the catalytic pyrolysis.[8,9] Different catalysts will cause different pyrolysis processes and change the compositions of the pyrolytic oil.[10−13] The molecular-sieve catalysts, including ZSM-5, MCM-41, and Y zoelite, are widely researched. Their different acidity and pore characteristics are the reasons for the variation of the final products.[12] The basic catalyst, known as the decarboxylation catalyst, can react with triglycerides to form fatty acid salts. Then, these fatty acid salts further decomposed into ketones and carbonates, thus producing the diesel-like fuels with a low acid value.[14]

Recently, the applications of molten salts in pyrolysis have been widely researched. Molten salt, referring to a salt or a mixture of several salts, is in the solid state at standard temperature and pressure (STP) and will melt into ionic liquid at high temperatures. Their special characters feature high heat capacities and good thermal stability at high temperatures, thus enabling them been used as the catalyst in thermal pyrolysis of biomass. The compositions of pyrolytic products would be different by varying proportion and amount of molten salts.[15] Kumar et al.[16] reported the activation of dehydrogenation of lower alkanes in molten alkali metal (Li, Na, and K) chlorides. The results showed that the high selectivity to ethene and propene was attributed to the high mobility of cations and anions. Molten alkali carbonates have also been widely used in coal–CO_2 gasification, and the experimental results demonstrated that the catalytic activity of intermixture carbonates was stronger than that of any single carbonate salt.[17] Furthermore, in the pyrolysis of rice stalk, Ai et al.[18] suggested that the $ZnCl_2$–KCl molten salt mixture had the capability of co-production, especially in activated carbon and bio-oil. On the other hand, Hsu et al.[19] reported a technology on recovery and reusage of molten salts, and this technology was mature and could be implemented in some commercial applications.

There was few study focusing on the catalytic pyrolysis of soybean oil to produce biofuels using molten salt. Thus, in this study, the thermogravimetric (TG) analysis was used to study the influence of the $ZnCl_2$–KCl molten salt mixture on soybean oil catalytic pyrolysis with/without the CaO catalyst. On the basis of the TG–differential thermogravimetric (DTG) curves, the pyrolysis experiments were carried out in a laboratory-scale continuous stirred tank reactor (CSTR, 1.5 L). The influences of the reaction temperature and CaO catalyst on the compositions and fuel properties of the bio-oil were studied.

2. EXPERIMENTAL SECTION

2.1. Materials. In this study, the soybean oil was commercially available and used without further treatment. The triglycerides are the main compositions in soybean oil. Nano CaO (purity of 99%) with a particle size of 160 nm was used as the basic catalyst. $ZnCl_2$ (purity of 98%), KCl (purity of 99.5%), and oleic acid (purity of 99%) were used in this study. The blend of $ZnCl_2$ and KCl with the mole ratio of 7:6 was selected because its melting point was 225 °C, much lower than each single chloride salt.[20] Additionally, the $ZnCl_2$–KCl molten salts had a high selectivity toward hydrocarbons.[15]

2.2. Methods. *2.2.1. TG Analysis.* About 8 mg of soybean oil was accurately used in each run. The amounts of CaO catalyst loaded were 0, 1.02, 1.53, and 2.68 mg. The $ZnCl_2$–KCl molten salts mixtur with a molar ratio of 7:6 was premixed with soybean oil in a beaker. The mass fraction of molten salts in the solid–liquid mixture was 33 wt %. Additionally, the CaO catalyst (about 11 wt %) was added to the solid–

Received: June 7, 2013
Revised: December 6, 2013
Published: December 6, 2013

liquid mixture to study its influence on the molten salt catalytic pyrolysis of soybean oil. The TG (NETZSCH, Germany) experiments were performed on the thermobalance, and the heating rate was 50 °C/min within the temperature range from 30 to 700 °C. At a constant flow rate of 20 mL/min, nitrogen (purity of 99.99%) was used as the carrier gas.

2.2.2. Apparatus and Procedure. The experiments were carried out under atmospheric pressure in a laboratory-scale CSTR (1.5 L). The schematic diagram of the molten salt pyrolysis system was depicted in Figure 1.

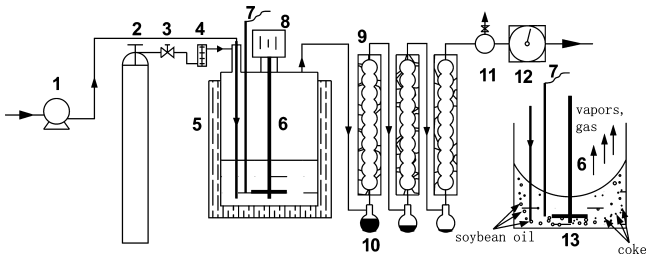

Figure 1. Schematic diagram of the molten salt pyrolysis system: (1) peristaltic pump, (2) gas cylinders, (3) reducing valve, (4) gas rotor flow meter, (5) heating jacket, (6) reactor, (7) thermocouples, (8) stirrer, (9) condenser pipe, (10) liquid product receiving bottle, (11) gas buffer bottle, (12) wet gas flow meter, and (13) schematic of the pyrolysis reaction that took place in the liquid phase.

At standard state, the densities of $ZnCl_2$ and KCl are 2.907 and 1.984 g/mL, separately. The weights of $ZnCl_2$ and KCl used in the study were 544.5 and 255.5 g, with the molar ratio of 7:6. Thus, the density of the $ZnCl_2$–KCl molten salt mixture was 2.61 g/mL. Theoretically, the available reaction volume for soybean oil pyrolysis was 306 mL ($^1/_5$ of the volume of the reacter). The $ZnCl_2$–KCl molten salt mixture was heated by an external electrical resistance. The thermocouple was inserted in the molten salts for continuous monitoring of the reaction temperature. Nitrogen (purity of 99.9%) was used as the carrier gas. When the melting point of the molten salts was reached, the stirring apparatus was switched on at the constant rotational speed of 200 revolutions/min. The carrier gas was ceased once the temperature rose to the present value. The soybean oil was added to the molten salts at the feed rate of 1.2 g/min by the peristaltic pump. The pyrolysis reaction took place in liquid phase immediately and formed products, including vapors (bio-oil and water), coke, and gas. The schematic of this reaction (13) was depicted in Figure 1. The vapors were cooled in the condenser pipe and collected in the liquid product receiving bottle. Once the reaction was completed, nitrogen was passed through again to purge the products of vapors and gas left in the reactor. Most of the vapors could be cooled in the condenser pipe and collected in the liquid product receiving bottle, while the volume of the gas product was difficult to calculate. Thus, the gas left in the reactor would be lost. In the liquid products, the water was separated from the bio-oil (BO) by the separating funnel. The remaining mixture in the reactor was then washed with water and filtered to recover the coke. In the presence of CaO catalyst, the HCl solution was used additionally to dissolve CaO and $CaCO_3$ and then washed with water to obtain the coke only. The equations used to calculate the yield of desired products (BO, water, gas, and coke) and conversion are as follows:

$$\text{yield (wt \%)} = \frac{\text{desired product (g)}}{\text{soybean oil feed (g)}} \times 100\% \quad (1)$$

$$\text{conversion (wt \%)} = \frac{[\text{BO (g)} + \text{water (g)} + \text{gas (g)} + \text{coke (g)}]}{\text{soybean oil feed (g)}} \times 100\% \quad (2)$$

In the same apparatus, the CaO catalyst was added to the molten salt mixture. The total amount of molten salts used in each experiment was 800 g, and the amounts of nano CaO added were 24 and 40 g, corresponding to the mass fraction of 3 and 5 wt %, respectively. CaO was uniformly dispersed in the molten salts by the stirring apparatus.

2.2.3. Product Analysis. Samples of the gas product were collected during the experiment. The samples were immediately analyzed in a gas chromatograph (Shimadzu, GC-2014). Helium with the purity of 99.999% was used as the carrier gas. The temperatures of injector and detector were both set at 120 °C for the thermal conductivity detector (TCD). For the flame ionization detector (FID), they were both set at 200 °C. The column temperature was set at 100 °C. Hydrocarbon components from C_1 to C_5 were conducted in a capillary column Pore-Q and detected by the FID. Other components were conducted in a packed column TDX-1 and detected by the TCD.

The gas chromatography–mass spectrometry (GC–MS, Agilent 7890A/5975C) analysis was conducted in a capillary column HP-5 (30 m × 250 μm × 0.25 μm). Helium with the purity of 99.999% was used as the carrier gas. To analyze the compositions of BO, the injector temperature was set at 280 °C. The oven temperature was started at 50 °C for 2 min and increased with the gradient of 3 °C/min to 200 °C for 5 min and 4 °C/min to 280 °C for 1 min. All of the peaks were determined with the help of the National Institute of Standards and Technology (NIST) library. Furthermore, some fuel properties were determined following standard procedures: density according to GB/T19147-2003, viscosity according to GB/T265-1988 on a viscosity determination device (ST265-2), and acid value according to GB/T264.[10]

3. RESULTS AND DISCUSSION

3.1. TG Analysis of Soybean Oil Pyrolysis with the CaO Catalyst. The TG–DTG curves of soybean oil pyrolysis with the CaO catalyst are shown in Figure 2. For comparison, the

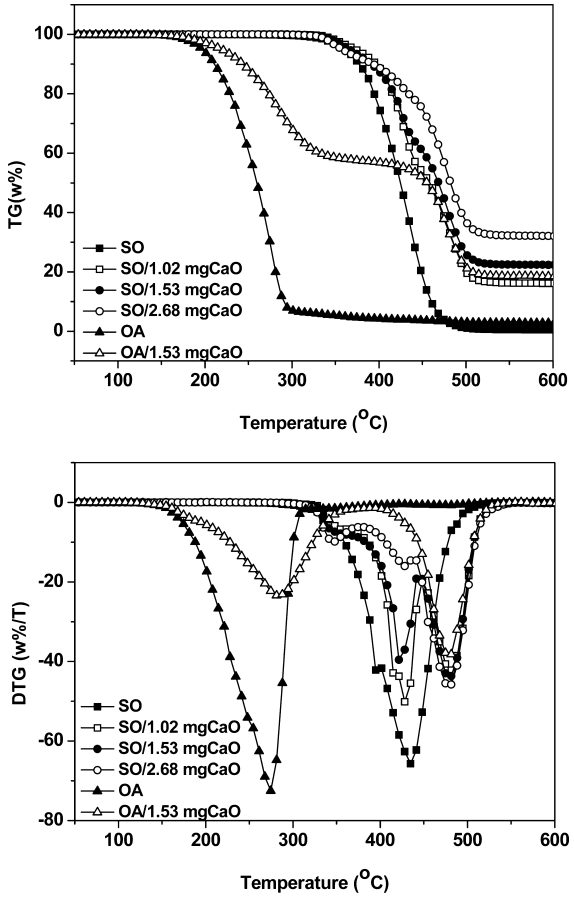

Figure 2. Influences of the CaO catalyst on the TG–DTG curves of soybean oil pyrolysis at 50 °C/min. SO = soybean oil, and OA = oleic acid.

dx.doi.org/10.1021/ef4015845 | *Energy Fuels* 2014, 28, 535–541

TG−DTG curves of pure soybean oil pyrolysis are also displayed. The pure soybean oil pyrolysis had only one distinct mass loss stage. However, after adding CaO, the TG−DTG curves exhibited two distinct mass loss stages. One appeared in the temperature range of 400−450 °C, and another one occurred between 450 and 500 °C. It indicated that the CaO catalyst could change the reaction pathway. The pyrolysis parameters are given in Table 1.

Table 1. Characteristic Parameters of Soybean Oil Pyrolysis[a]

experiments	CaO (mg)	T_{max1} (°C)	T_{max2} (°C)	$(dw/dT)_{max1}$ (wt %/°C)	$(dw/dT)_{max2}$ (wt %/°C)
1	0	433		−65.69	
2	1.02	430	479	−50.52	−42.35
3	1.53	423	480	−41.93	−44.05
4	2.68	426	479	−16.16	−46.60

[a] T_{max1}, temperature of the first maximum mass loss step; T_{max2}, temperature of the second maximum mass loss step; $(dw/dT)_{max1}$, maximum mass loss rate at T_{max1}; and $(dw/dT)_{max2}$, maximum mass loss rate at T_{max2}.

Obviously, with 1.02 mg of CaO catalyst, the maximum mass loss rate at T_{max1} decreased from 65.69 to 50.52% compared to that of pure soybean oil pyrolysis. When the amount of CaO catalyst increased to 2.68 mg, the maximum mass loss rate at T_{max1} decreased from 50.52 to 16.16%, while the maximum mass loss rate at T_{max2} increased from 42.35 to 46.60%. These were partially owing to the CaO carbonation reaction, through which the CaO catalyst absorbed CO_2 to form $CaCO_3$.[21] This viewpoint could also be verified from the TG−DTG curves of oleic acid (as shown in Figure 2). The reaction pathway of pure oleic acid pyrolysis was changed in the presence of the CaO catalyst. In the TG−DTG curves, the first mass loss step appeared in almost the same temperature range as pure oleic acid pyrolysis. The second mass loss step occurred at higher temperatures (450−500 °C) for calcium oleate pyrolysis. It revealed that the CaO catalyst has reacted with oleic acids to form metal salts. Then, the metal salts further decomposed into ketones and hydrocarbons at high temperatures (450−500 °C).[14] The proposed reaction pathways were presented in Figure 4 (reactions 5a−5d).

In molten salt catalytic pyrolysis of soybean oil, the TG−DTG curves (Figure 3) displayed three mass loss steps between 200 and 500 °C, while in the curves of a sole molten salt mixture, there was no mass loss step between 200 and 500 °C. The mass loss step between 500 and 700 °C was caused by the exudation of salts, which could be observed after the TG experiment. In catalytic pyrolysis of soybean oil, the first mass loss step started at 225 °C, which was the melting point of the $ZnCl_2$−KCl molten salt mixture.[20] This change might be caused by the decomposition of triglycerides in the presence of molten salts and formed fatty acids, aldehydes, ketones, and hydrocarbons (reactions 1a−1d in Figure 4).[13] The other two mass loss steps appeared between 400 and 500 °C. Zou et al.[22] reported that the chlorides of alkali earth metal and transition metal had different catalytic mechanisms during the coal pyrolysis process. The chlorides of alkali earth metal linked with an oxygen-bearing free radical (such as a carboxyl or hydroxide) to form a virtual cross-linking point, while the chlorides of transition metal transformed into metal oxide and HCl in the presence of water. Branco et al.[15] reported that, before reaction, the $ZnCl_2$−KCl molten salt mixture have formed $K_2Zn_2Cl_4$, an eutectic type. After reaction,

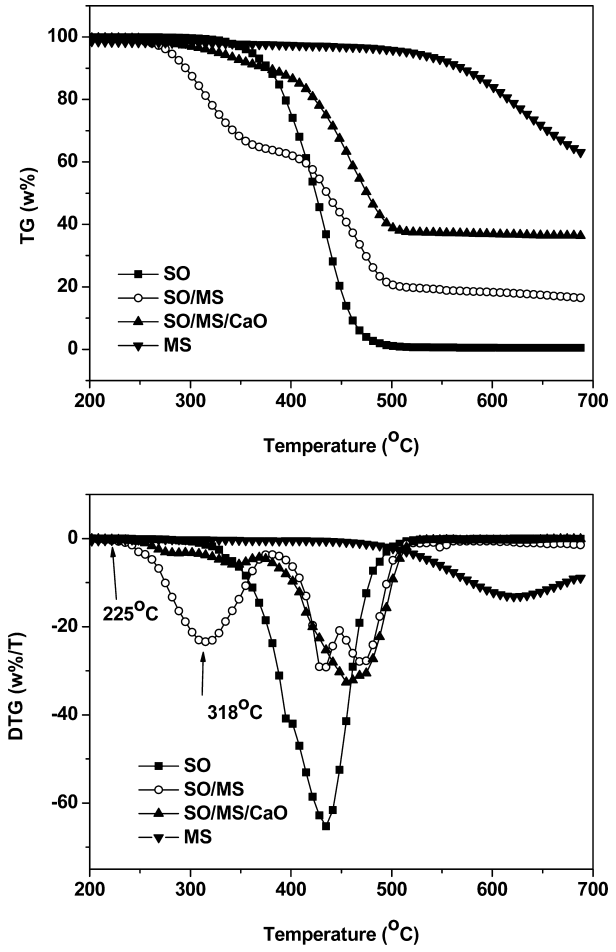

Figure 3. TG−DTG curves of the molten salt catalytic pyrolysis of soybean oil with/without CaO catalyst. The heating rate was 50 °C/min. SO = soybean oil, and MS = molten salt.

the powder X-ray diffraction (XRD) analysis revealed the presence of ZnO, which implied that $ZnCl_2$ had transformed into ZnO. Thus, in this study, the compounds containing carboxyl or hydroxide linked with the potassium ions repeatedly and then decomposed into hydrocarbons (reactions 3a and 3b), [23] while Cl^- was released from $ZnCl_2$ as HCl during soybean oil pyrolysis and lead to the formation of ZnO (reaction 4a).[24] Subsequently, ZnO combined with fatty acid and formed fatty acid zinc, which then further decomposed into ZnO and hydrocarbons at the temperature between 400 and 450 °C.[25,26] In addition, $ZnCl_2$ could be generated from the reductive action in the presence of hydrogen or carbon monoxide (reaction 4d).[22] Thus, the second mass loss step of soybean oil pyrolysis was attributed to the pyrolysis of fatty acid zinc (reactions 4b−4d). Moreover, the third mass loss step might be attributed to the pyrolysis of fatty acid potassium (reactions 3a and 3b). In summary, the pyrolysis of soybean oil was carried out in advance in the presence of molten salts and formed fatty acid salts (fatty acid zinc and fatty acid potassium, reactions 3a and 4b).[26,22] In the temperature range of 400−500 °C, these fatty acid salts further decomposed into hydrocarbons (reactions 3b and 4c).[13]

After adding CaO to the molten salt mixture, the TG−DTG curves of soybean oil were significantly changed. The first mass loss step became flat, and the latter two steps nearly turned into only one step. These were owing to the carbonation of CaO. To explain such a result, the enthalpy changes (at 430 and 455 °C) of

dx.doi.org/10.1021/ef4015845 | Energy Fuels 2014, 28, 535−541

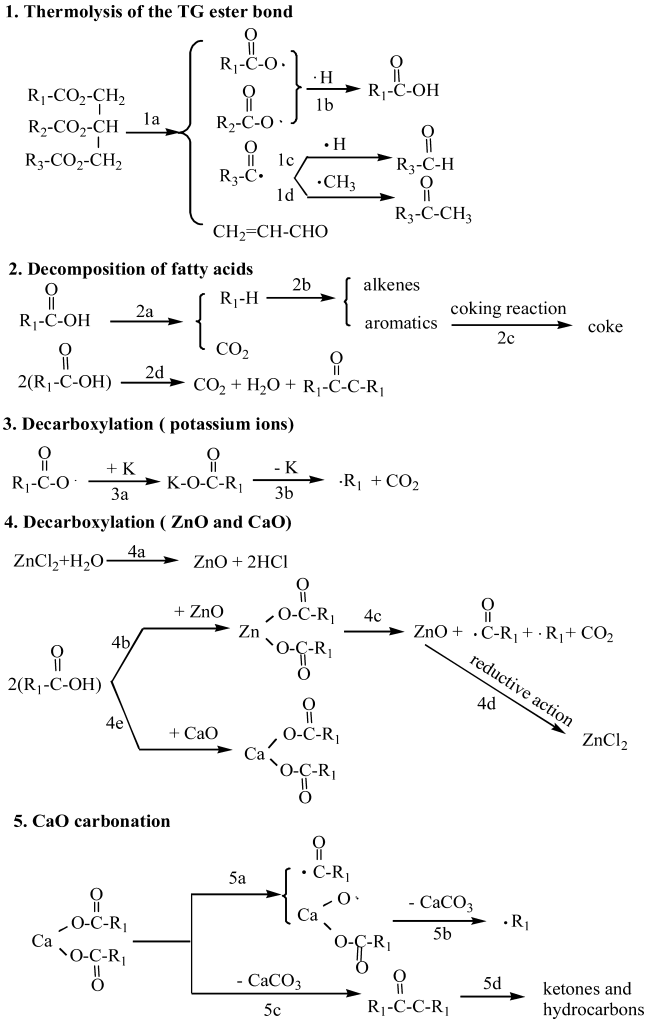

Figure 4. Mechanism proposed on catalytic pyrolysis of soybean oil.

metal oxide carbonation are listed in eqs 3 and 4. It shows that CaO carbonation had a much lower enthalpy change than that of ZnO carbonation. That is to say, CaO was easier to react with fatty acids and form calcium carbonate than that of ZnO. Additionally, CaO as a basic catalyst also had the priority to combine with fatty acids than that of KCl.

$$CaO + CO_2 = CaCO_3, \quad \Delta H_{430} = -177.47\ \text{kJ/mol}, \quad \Delta H_{455} = -177.42\ \text{kJ/mol} \tag{3}$$

$$ZnO + CO_2 = ZnCO_3, \quad \Delta H_{430} = -69.98\ \text{kJ/mol}, \quad \Delta H_{455} = -69.92\ \text{kJ/mol} \tag{4}$$

In a word, the reaction mechanism was put forward by TG experiments of soybean oil catalytic pyrolysis. The mass loss steps indicated that the temperature in pyrolysis should be controlled between 400 and 500 °C. In addition, a high decomposition temperature could promote the internal ion mobility and increase the catalytic activity.[15,16] A high catalyst concentration could promote the contact between metal cations and soybean oil and promote the decarboxylation. Thus, the production process could be considered as pyrolysis, and the appropriate pyrolysis reactor selected was CSTR.

3.2. Results of Catalytic Pyrolysis Experiments. *3.2.1. Influences of the Reaction Temperature and CaO Catalyst on Pyrolysis.* The pyrolytic temperature was set between 430 and 505 °C. The amounts of CaO catalyst loaded were 3 and 5 wt % to the total amount of the molten salt mixture. The products of BO, water, coke, and gas were generated after soybean oil pyrolysis. The influences of the reaction temperature and CaO catalyst on molten salt catalytic pyrolysis were investigated in the CSTR. The product distribution and fuel properties of the BO are shown in Tables 2 and 3, respectively. Within the tables, 430[a] and 430[b] °C showed the reproducibility of this pyrolysis facility. Moreover, the data of non-catalytic pyrolysis was also listed to explain the role of the molten salt mixture and CaO catalyst.

In this study, the mass balance of 430[b] °C was soybean oil pumped (60.4 g) = vapor [bio-oil (35.1 g) + water (2.2 g)] + gas (9.3 g) + coke (11.0 g) + loss (2.8 g). The loss included gas (left in the reactor), liquid (left in the reactor and condenser pipe), and coke (left in the reactor and lost when filtered).

It can be seen from Table 2 that, at the temperature of 430 °C, the BO yield of non-catalytic pyrolysis was more than that of molten salt catalytic pyrolysis, while the yields of coke and gas were less. Furthermore, the acid value (as shown in Table 3) and selective ion chromatogram (SIC) of fatty acids (as shown in chromatogram B_1 of Figure 5) suggested that, in the absence of catalyst, the pyrolysis of fatty acids was not complete when compared to that of catalytic pyrolysis. This indicated that the molten salts could promote the decarboxylation of fatty acids and

Table 2. Product Distribution of the Molten Salt Catalytic Pyrolysis of Soybean with/without CaO Catalyst

			yield of products (wt %)					distribution of BO (wt %)	
T (°C)	CaO (wt %)	RT[a] (min)	BO	water	coke	gas	conversion	HC[b]	OC[c]
430	non-catalytic	3.5	66.0	4.0	11.8	8.9	90.7	55.1	10.9
430[a]	0	2.6	56.9	3.6	18.9	14.9	94.3		
430[b]	0	2.5	58.1	3.6	18.2	15.4	95.2	51.3	6.8
455	0	2.1	59.9	2.9	16.4	16.7	96.0	51.7	8.2
480	0	1.8	60.6	1.9	14.0	20.6	97.0	48.3	12.3
505	0	1.6	61.0	0.8	12.5	22.4	96.6	47.4	13.6
430	3	2.5	61.3	2.9	16.0	15.1	95.3	50.7	10.6
455	3	2.1	61.0	2.5	15.9	16.1	95.5	48.4	12.6
430	5	2.4	60.3	2.8	14.0	17.7	94.8	48.9	11.4
455	5	2.0	60.9	2.3	14.8	18.7	96.6	46.6	14.3

[a]RT = residence time of soybean oil in molten salts based on the quantity of the gas flow rate measured after the reaction has taken place in the molten salts. [b]HC = hydrocarbon. [c]OC = oxygen-containing compound. Both yields calculated from the chromatographic analysis of bio-oil.

dx.doi.org/10.1021/ef4015845 | *Energy Fuels* 2014, 28, 535−541

Table 3. Fuel Properties of the Bio-oils

		BO properties		
T (°C)	CaO (wt %)	density (kg/m^3)	kinematic viscosity (20 °C, mm^2/s)	acid value (mg of KOH/g)
430	non-catalytic	810.3	1.73	89.0
430[a]	0	822.1	2.60	6.6
430[b]	0	827.5	2.91	6.7
455	0	839.5	3.41	17.4
480	0	859.4	6.65	22.4
505	0	863.9	7.47	26.7
430	3	830.4	3.12	4.8
455	3	844.2	3.62	10.0
430	5	837.8	3.71	3.9
455	5	846.9	4.02	5.6
soybean oil		913.7	61.3[a]	
biodiesel[b]		860−900[c]	1.9−6.0	0.8

[a]Measured at 40 °C. [b]According to ASTM 6751-03. [c]According to EN 14214:2005.

the pyrolysis of soybean oil was relatively full. Moreover, the density and kinematic viscosity (as shown in Table 3) of BO generated from non-catalytic pyrolysis were much lower than that of catalytic pyrolysis. Otherwise, in comparison to the catalytic pyrolysis (as shown in Table 5), the non-catalytic pyrolysis was in favor of the formation of hydrocarbons between C_6 and C_{14} rather than between C_{15} and C_{20}. On this basis, we came to a conclusion that there are some relationships between the chain length of hydrocarbons and fuel properities.

Table 2 shows that the temperature had great influence on the formation of coke (reaction 2c) and gas. The higher the temperature, the greater the gas yield while the lower the coke yield. On the other hand, with the increase of the gas yield, the residence time of soybean oil in molten salts was reduced. The BO generated from catalytic pyrolysis was the main product, accounting for 56.9−61.0%, and varied slightly with the temperature. The difference of BO and coke yields between 430[a] and 430[b] °C might be caused by the residual products in the condenser pipe and reactor, respectively. The total oxygen-containing compounds increased from 6.8 to 13.6% with the increasing temperature, while the yields of water decreased from 3.6 to 0.8%. It implied that the effect of deoxygenation was not complete at high temperatures. Branco et al.[15] reported that a high reaction temperature could promote the internal ion mobility and increase the gas yield. However, the enthalpy changes (at 430 and 455 °C) of metal oxide carbonation (as shown in eqs 3 and 4) revealed that both the enthalpy changes increased with the increase of the temperature. That is to say, the effect of decarboxylation was weakened at higher temperatures. Moreover, high temperatures also reduced the residence time, which might promote the vaporization of heavy organic materials.[27] Thus, the acid value increased from 6.7 to 26.7 mg of KOH/g with the increase of the temperature. Additionally, the density and kinematic viscosity also increased (as shown in Table 3).

After adding CaO to the molten salts, the gas yield increased, which could be associated with the composition distribution data of bio-oil (Table 5). Because CaO promoted the pyrolysis of hydrocarbons between C_9 and C_{14}, the formation of hydrocarbons between C_6 and C_8 increased, as well as the gas yield. The TG experiments revealed that, first, the CaO catalyst would react with fatty acids to form fatty acid salts. Then the fatty acid

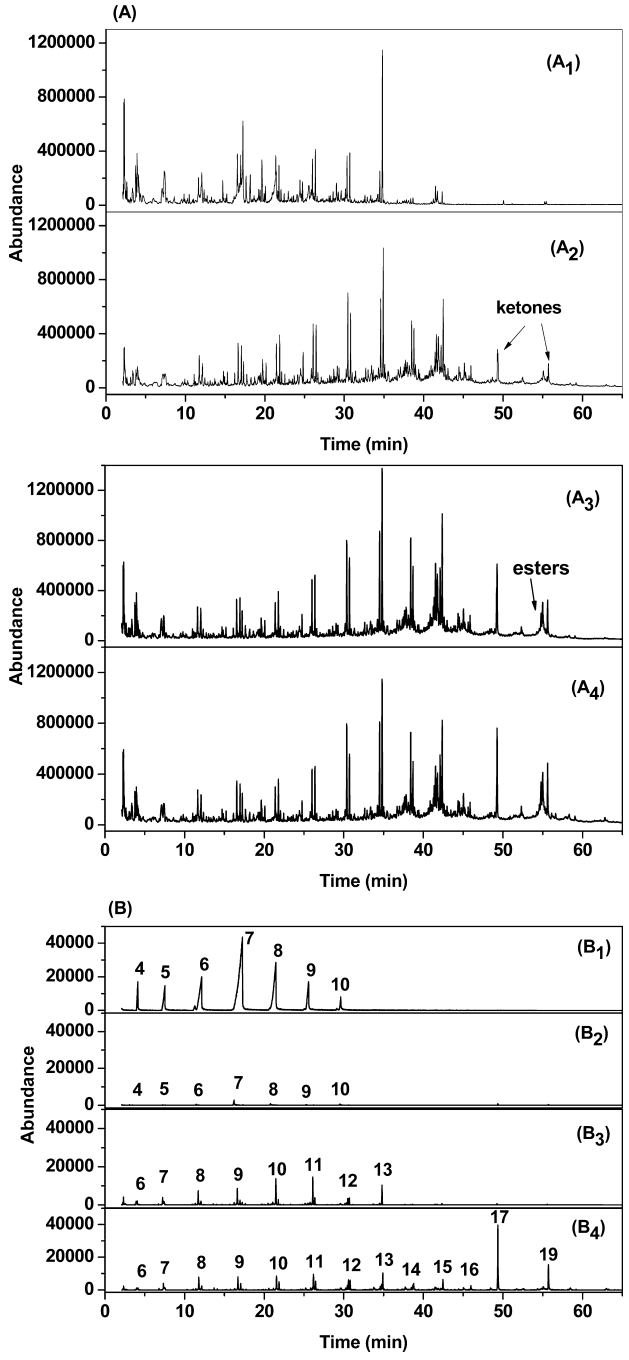

Figure 5. (A) TIC of BO obtained through non-catalytic pyrolysis (A_1) and molten salt catalytic pyrolysis with 0 wt % CaO (A_2), 3 wt % CaO (A_3), and 5 wt % CaO (A_4). (B) SIC of fatty acids (B_1 and B_2, m/z 60) and ketones (B_3 and B_4, m/z 58) generated from non-catalytic pyrolysis (B_1 and B_3) and molten salts catalytic pyrolysis (B_2 and B_4) at 430 °C, respectively. The numbers shown in the chromatograms correspond to the number of carbon atoms for each compound.

salts further decomposed into hydrocarbons.[14,25,28] At the temperature of 430 °C, with an increasing amount of CaO catalyst, the CaO carbonation reaction was intensified and the acid value of BO was decreased. The acid value decreased from 6.7 to 4.8 mg of KOH/g when using 3 wt % CaO and further decreased to 3.9 mg of KOH/g when the addition of CaO catalyst was 5 wt %. Although the CaO catalyst could reduce the acid value, the density and kinematic viscosity still increased, significantly. It indicated that the pyrolysis reaction in the CSTR

dx.doi.org/10.1021/ef4015845 | Energy Fuels 2014, 28, 535−541

should be carried out at a relatively low temperature (430 °C) and the amount of CaO catalyst was 5 wt % to obtain the bio-oil with a lower acid value.

3.2.2. Chromatographic Analysis of the Gas Product. Samples of gas products were analyzed by the gas chromatograph, and the gas compositions of non-catalytic pyrolysis and molten salt catalytic prolysis of soybean oil at 430 °C are shown in Table 4.

Table 4. Main Components in Gas Products at 430 °C

	percentage (mol %)	
composition	non-catalytic pyrolysis	catalytic prolysis
H_2	30.75	24.40
CO	36.43	13.84
CO_2	20.12	40.48
CH_4	3.01	6.07
C_2H_6	2.66	4.14
C_2H_4	1.82	2.24
C_3H_8	2.00	2.85
C_4H_8	0.43	1.22
C_5H_{12}	2.77	4.74
C_5H_{10}	0.01	0.03

It can be seen from Table 4 that the gas yield of molten salt catalytic pyrolysis was more than that of non-catalytic pyrolysis, which indicated that the catalytic pyrolysis of soybean oil was relatively thorough. In the gas mixture, H_2, CO, and CO_2 were the main compounds. For non-catalytic pyrolysis, the formation of CO was dominated, while CO_2 was the main component in molten salt catalytic pyrolysis. The formation of CO and CO_2 were obviously different according to the two reaction mechanisms, which are shown as follows:

$$R{-}COOH \rightarrow R{-}H + CO_2 \quad (5)$$

$$R_1{-}CO{-}R_2 \rightarrow R_1{-}R_2 + CO \quad (6)$$

From Figure 5 (B_3 and B_4) and Table 5, it can be seen that, in the absence of the catalyst, decarbonylation (eq 6) was dominated and the formation of ketones was less than that of the catalytic pyrolysis. Nevertheless, decarboxylation (eq 5) was relatively weak, and the content of fatty acids (as shown in chromatograms B_1 and B_2 of Figure 5 and Table 5) and the acid value (as shown in Table 3) were higher than that of the catalytic pyrolysis. In the presence of molten salts, the reaction mechanism of decarboxylation could be interpreted as reactions 3b and 4c (as shown in Figure 4).

The mole fractions of hydrocarbons from C_1 to C_5 were in the order of $CH_4 > C_5H_{12} > C_2H_6 > C_3H_8 > C_2H_4 > C_4H_8 > C_5H_{10}$. In molten salt catalytic pyrolysis, the mole fractions of hydrocarbons were generally higher than those of non-catalytic pyrolysis. It implied that the catalytic pyrolysis was in favor of the formation of hydrocarbons. Moreover, it was much easer for unsaturated hydrocarbons to form saturated hydrocarbons by hydrogen-transfer reaction on the catalyst.[9]

3.2.3. Chromatographic Analysis of Bio-oil. Samples of BO obtained from soybean oil pyrolysis in the absence and presence of catalysts were analyzed by GC−MS. Figure 5 shows the total ion chromatogram (TIC) and SIC of BO. Chromatograms unfolding were carried out in the same time, and nearly 170 peaks were identified, with a relative concentration higher than 0.05%. The compositions were quantified by the area normalization method, and the distribution data of the BO obtained at 430 °C are shown in Table 5.

Table 5. Composition Distribution Data of the Bio-oil Obtained at 430 °C

			thermal catalytic pyrolysis		
			CaO in the mixture of molten salts (wt %)		
distribution (wt %)		non-catalytic pyrolysis	0	3	5
alkanes	C_{6-8} linear	5.1	2.0	2.8	2.8
	C_{9-14} linear	13.2	8.3	7.6	7.2
	C_{15-20} linear	5.1	11.1	11.4	11.5
	total linear	23.3	21.4	21.7	21.4
	cycloalkanes	2.8	4.2	3.9	3.4
	total	26.2	25.6	25.7	24.8
alkenes	C_{6-8} linear	7.3	3.1	4.0	4.3
	C_{9-14} linear	24.4	15.4	11.7	12.1
	C_{15-20} linear	4.4	19.2	21.6	17.9
	total lines	36.1	37.6	37.3	34.3
	cycloolefin	8.6	9.0	6.6	7.3
	total	44.7	46.6	43.9	41.6
aromatics	total	12.6	16.1	13.2	12.7
alcohols	total	1.5	1.4	3.3	2.9
aldehydes	total	1.0	1.9	2.0	2.0
ketones	total	1.5	3.8	6.3	7.4
esters	total	0.5	1.8	4.2	7.6
fatty acids	total	12.1	2.9	1.5	0.9
OC	total	16.5	11.7	17.3	20.8

In the chromatograms (as shown in Figure 5A) of the bio-oils obtained through non-catalytic pyrolysis (A_1) and molten salt catalytic pyrolysis (A_2), there was a significant difference in the distribution of compositions. As shown in Table 5, when compared to the catalytic pyrolysis, the non-catalytic pyrolysis was in favor of the formation of hydrocarbons between C_6 and C_{14} rather than between C_{15} and C_{20}. It means that, in the presence of the catalyst, the light components in BO have transformed into gaseous hydrocarbon. It is been proven in Table 4 that the mole fractions of hydrocarbons in the gas product were generally higher than those of non-catalytic pyrolysis. The changes of ketones and fatty acids could be associated with those of the gas products (CO and CO_2), which have been discussed in the above section.

Chromatogram A_2 of Figure 5 shows that the $ZnCl_2$−KCl molten salt mixture had the potential to generate fuels with a chemical composition similar to that of petroleum-based fuels. The hydrocarbons were the main part of the BO, which accounted for 88.3%. Meanwhile, Table 5 shows that the alkenes were the main components, which accounted for 46.6%. These alkenes could be transformed into alkanes through hydrogenation reaction, and the quality of BO could be promoted, ultimately. After the CaO catalyst was added, there was a significant increase in the peaks of long-chain esters (Figure 5A). It implied that the pyrolysis of esters was not complete at this state. The peaks of ketones (C_{17} and C_{19} in chromatograms A_3 and A_4 of Figure 5) were also increased with the increasing amount of CaO catalyst, which could also be verified from Table 5. With the increasing amount of CaO catalyst, the total ketones increased from 3.8 to 7.4%. Zou et al.[22] reported that Ca could enhance the polymerization reaction between macromolecular free radicals. In soybean oil pyrolysis, Ca promoted the formation

dx.doi.org/10.1021/ef4015845 | Energy Fuels 2014, 28, 535−541

of ketones (reaction 5c). Besides, during saponification, the strong electron-withdrawing group (alkali metal) reacted with fatty acids, which promoted the decarboxylation reaction (reactions 4c and 5a)[29,30] and resulted in the decrease of total fatty acids from 2.9% (without CaO) to 0.9% (with 5 wt % CaO) (Table 5). The CaO catalyst also could accelerate the rupture of ringed structures.[31,32] In Table 5, the relative concentration of aromatics decreased along with the cycloalkanes. At 5 wt % of CaO catalyst, the total aromatics and cycloalkanes decreased from 16.1% and 4.2% to 12.7% and 3.4%, respectively.

In summary, using the $ZnCl_2$−KCl molten salt mixture as the catalyst on soybean oil pyrolysis was feasible. The decarboxylation was dominated when compared to non-catalytic pyrolysis. The CaO catalyst had the ability not only to decrease the acid value but also to accelerate the rupture of ringed structures.

4. CONCLUSION

To study the mechanism of molten salt catalytic pyrolysis of soybean oil, the TG experiments were carried out. The TG−DTG curves revealed that the soybean oil formed fatty acid salts (fatty acid zinc and fatty acid potassium) in the presence of molten salts. At high temperatures (400−500 °C), these fatty acid salts further decomposed into hydrocarbons. The pyrolysis experiments were carried out in the CSTR. It revealed that the $ZnCl_2$−KCl molten salt mixture with the CaO catalyst had the potential to produce diesel-like fuels with a low acid value, which was 3.9 mg of KOH/g at 5 wt % of CaO catalyst. Additionally, the CaO catalyst could accelerate the rupture of ringed structures and lead to the decrease of total aromatics and cycloalkanes. However, the CaO catalyst inhibited the pyrolysis of esters and lead to the increase of total oxygen-containing compounds.

■ ASSOCIATED CONTENT

Supporting Information

Detailed reaction process of soybean oil in CSTR, choice of the concentration of the molten salt mixture, bio-oil refining by the hydrogenation reaction (Figure S1), TIC of bio-oil generated in molten salt catalytic pyrolysis at 455, 480, and 505 °C (Figure S2), and TIC of bio-oil generated in molten salt catalytic pyrolysis with 3 and 5% CaO catalyst at 455 °C (Figure S3). This material is available free of charge via the Internet at http://pubs.acs.org.

■ AUTHOR INFORMATION

Corresponding Author

*E-mail: yufw@zjut.edu.cn.

Notes

The authors declare no competing financial interest.

■ ACKNOWLEDGMENTS

The authors are very grateful to the Doctoral Fund of the Ministry of Education of China (Grant 20103317110001) and the Zhejiang Key Innovation Team of Clean Utilization of Biomass Energy (Grant 2009R50012).

■ REFERENCES

(1) Mauzerall, D. L.; Sultan, B.; Kim, N.; Bradford, D. F. *Atmos. Environ.* **2005**, *39* (16), 2851−2866.
(2) Huber, G. W.; Iborra, S.; Corma, A. *Chem. Rev.* **2006**, *106* (9), 4044−4098.
(3) Bhatia, S.; Mohamed, A. R.; Shah, N. A. A. *Chem. Eng. J.* **2009**, *155* (1−2), 347−354.
(4) Zhu, J. H.; Wei, S. Y.; Li, Y. F.; Pallavkar, S.; Lin, H. F.; Haldolaarachchige, N.; Luo, Z. P.; Young, D. P.; Guo, Z. H. *J. Mater. Chem.* **2011**, *21*, 16239−16246.
(5) Zhang, Y. N.; Brown, T. R.; Hu, G. P.; Brown, R. C. *Chem. Eng. J.* **2013**, *225* (1), 895−904.
(6) Sharma, B. K.; Suarez, P. A. Z.; Perez, J. M.; Erhan, S. Z. *Fuel Process. Technol.* **2009**, *90* (10), 265−1271.
(7) Lin, H. F.; Strull, J.; Liu, Y.; Karmiol, Z.; Plank, K.; Miller, G.; Guo, Z. H.; Yang, L. S. *Energy Environ. Sci.* **2012**, *5* (12), 9773−9777.
(8) Uzun, B. B.; Sarioğlu, N. *Fuel Process. Technol.* **2009**, *90* (5), 705−716.
(9) Li, H.; Yu, P. H.; Shen, B. X. *Fuel Process. Technol.* **2009**, *90* (9), 1087−1092.
(10) Xu, J. M.; Jiang, J. C.; Sun, Y. J.; Chen, J. *Bioresour. Technol.* **2010**, *101*, 9803−9806.
(11) Zhu, J. H.; Gu, H. B.; Rapole, S. B.; Luo, Z. P.; Pallavkar, S.; Haldolaarachchige, N.; Benson, T. J.; Ho, T. C.; Hopper, J.; Young, D. P.; Wei, S. Y.; Guo, Z. H. *RSC Adv.* **2012**, *2* (11), 4844−4856.
(12) Chew, T. L.; Bhatia, S. *Bioresour. Technol.* **2009**, *100* (9), 2540−2545.
(13) Maher, K. D.; Bressler, D. C. *Bioresour. Technol.* **2007**, *98* (12), 2351−2368.
(14) Yang, X. L.; Zhang, J.; Zhu, X. F. *Energy Fuels* **2008**, *22* (4), 2598−2603.
(15) Branco, J. B.; Lopes, G.; Ferreira, A. C.; Leal, J. P. *J. Mol. Liq.* **2012**, *171*, 1−5.
(16) Kumar, C. P.; Gaab, S.; Muller, T. E.; Lercher, J. A. *Top. Catal.* **2008**, *50*, 156−167.
(17) Jin, G.; Iwaki, H.; Arai, N.; Kitagawa, K. *Energy* **2005**, *30*, 1192−1203.
(18) Ai, N.; Zeng, G. N.; Zhou, H. Y. *Bioresources* **2013**, *8* (2), 1551−1562.
(19) Hsu, P. C.; Foster, K. G.; Ford, T. D.; Wallman, P. H.; Watkins, B. E.; Pruneda, C. O.; Adamson, M. G. *Waste Manage.* **2000**, *20*, 363−368.
(20) Kudsy, M.; Kumazawa, H. *Can. J. Chem. Eng.* **1999**, *77* (6), 1176−1184.
(21) Han, L.; Wang, Q. H.; Ma, Q.; Yu, C. J.; Luo, Z. Y.; Cen, K. F. *J. Anal. Appl. Pyrolysis* **2010**, *88* (2), 199−206.
(22) Zou, X. W.; Yao, J. Z. X.; Yang, M.; Song, W. L.; Lin, W. G. *Energy Fuels* **2007**, *21* (2), 619−624.
(23) Kubátová, A.; Luo, Y.; Štávová, J.; Sadrameli, S. M.; Aulich, T.; Kozliak, E.; Seames, W. *Fuel* **2011**, *90* (8), 2598−2608.
(24) Quyn, D. M.; Wu, H. W.; Li, C. Z. *Fuel* **2002**, *81* (2), 143−149.
(25) Tang, W. J.; Chen, D. H. *Powder Technol.* **2008**, *181*, 343−346.
(26) Chiavari, C.; Fabbri, D.; Prati, S. *J. Anal. Appl. Pyrolysis* **2005**, *74* (1−2), 39−44.
(27) Luo, Y.; Ahmed, I.; Kubátová, A.; Šťávová, J.; Aulich, T.; Sadrameli, S. M.; Seames, W. S. *Fuel Process. Technol.* **2010**, *91* (6), 613−617.
(28) Xu, J. M.; Jiang, J. C.; Chen, J.; Sun, Y. J. *Bioresour. Technol.* **2010**, *101* (14), 5586−5591.
(29) Lappi, H.; Alén, R. *J. Anal. Appl. Pyrolysis* **2009**, *86* (2), 274−280.
(30) Lappi, H.; Alén, R. *J. Anal. Appl. Pyrolysis* **2011**, *91* (1), 154−158.
(31) Jia, Y. B.; Huang, J. J.; Wang, Y. *Energy Fuels* **2004**, *18* (6), 1625−1632.
(32) Jordan, C. A.; Akay, G. *Fuel Process. Technol.* **2013**, *106*, 654−660.

■ NOTE ADDED AFTER ASAP PUBLICATION

This article published December 13, 2013 missing the top portion of Figure 5. The correct version published January 16, 2014.